Research Article | Vol. 7, No. 1 | 1 Jan 2017 | OPTICAL MATERIALS EXPRESS 133

Optical Materials EXPRESS

Peristrophic multiplexed holograms recorded in a low toxicity photopolymer

VÍCTOR NAVARRO-FUSTER,[1,2,*] MANUEL ORTUÑO,[2,3] ROBERTO FERNÁNDEZ,[2,3] SERGI GALLEGO,[2,3] ANDRÉS MÁRQUEZ,[2,3] AUGUSTO BELÉNDEZ,[2,3] AND INMACULADA PASCUAL[1,2]

[1]*Departamento de Óptica, Farmacología y Anatomía, Universidad de Alicante, Apartado 99, 03080, Alicante, Spain*
[2]*Instituto Universitario de Física Aplicada a las Ciencias y las Tecnologías, Universidad de Alicante, Apartado 99, 03080, Alicante, Spain*
[3]*Departamento de Física, Ingeniería de Sistemas y Teoría de la Señal, Universidad de Alicante, Apartado 99, 03080, Alicante, Spain*
**victor.navarro@ua.es*

Abstract: Multiplexed diffraction gratings were recorded in 300 μm thick layers of biophotopol photopolymer by using two peristrophic multiplexing schemes separately and in combination. In addition, it was shown that riboflavin may be used as polymer initiator in acrylamide photopolymer films and the holographic properties of these films such as diffraction efficiency and dynamic range were compared with those of the biophotopol photopolymer. A variable exposure scheduling method was adopted to store the gratings using a 488 nm Ar laser. Thirteen nearly uniform sinusoidal wave gratings could be recorded in a low toxicity recording medium with a variable exposure energy scheduling method. The diffraction efficiency and dynamic range obtained using the two multiplexing schemes were compared.

OCIS codes: (090.4220) Multiplex holography; (210.4810) Optical storage-recording materials; (160.4670) Optical materials; (160.1435) Biomaterials.

References and links

1. H. Ruan, "Recent advances in holographic data storage," Front. Optoelectron. **7**(4), 450–466 (2014).
2. F.-K. Bruder, R. Hagen, T. Rölle, M.-S. Weiser, and T. Fäcke, "From the surface to volume: concepts for the next generation of optical-holographic data-storage materials," Angew. Chem. Int. Ed. Engl. **50**(20), 4552–4573 (2011).
3. K. Anderson, M. Ayres, F. Askham, and B. Sissom, "Holographic data storage: Science fiction or science fact?" Proc. SPIE **9201**, 920102 (2014).
4. J. Marín-Sáez, J. Atencia, D. Chemisana, and M.-V. Collados, "Characterization of volume holographic optical elements recorded in Bayfol HX photopolymer for solar photovoltaic applications," Opt. Express **24**(6), A720–A730 (2016).
5. M. V. Collados, D. Chemisana, and J. Atencia, "Holographic solar energy systems: The role of optical elements," Renew. Sustain. Energy Rev. **59**, 130–140 (2016).
6. F.-K. Bruder, H. Bang, T. Fäcke, R. Hagen, D. Hönel, E. Orselli, C. Rewitz, T. Rölle, D. Vukicevic, and G. Walze, "Precision holographic optical elements in Bayfol HX photopolymer," Proc. SPIE **9771**, 977103 (2016).
7. N. K. Mohan, Q. T. Islam, and P. K. Rastogi, "Recent developments in holographic optical elements (HOEs)," Opt. Lasers Eng. **44**, 871–880 (2006).
8. A. Olivares-Pérez, M. P. Hernández-Garay, I. Fuentes-Tapia, and J. C. Ibarra-Torres, "Holograms in polyvinyl alcohol photosensitized with $CuCl_2 2H_2O$," Opt. Eng. **50**(6), 065801 (2011).
9. D. Cody, I. Naydenova, and E. Mihaylova, "New non-toxic holographic photopolymer material," J. Opt. **14**(1), 015601 (2012).
10. D. Cody, S. Gribbin, E. Mihaylova, and I. Naydenova, "Low-Toxicity Photopolymer for Reflection Holography," ACS Appl. Mater. Interfaces **8**(28), 18481–18487 (2016).
11. M. Ortuño, S. Gallego, A. Márquez, C. Neipp, I. Pascual, and A. Beléndez, "Biophotopol: A Sustainable Photopolymer for Holographic Data Storage Applications," Materials (Basel) **5**(12), 772–783 (2012).
12. V. Navarro-Fuster, M. Ortuño, S. Gallego, A. Márquez, A. Beléndez, and I. Pascual, "Biophotopol's energetic sensitivity improved in 300 μm layers by tuning the recording wavelength," Opt. Mater. **52**, 111–115 (2016).
13. N. Beztsinna, M. Solé, N. Taib, and I. Bestel, "Bioengineered riboflavin in nanotechnology," Biomaterials **80**, 121–133 (2016).

#278532 http://dx.doi.org/10.1364/OME.7.000133
Journal © 2017 Received 11 Oct 2016; revised 28 Nov 2016; accepted 28 Nov 2016; published 8 Dec 2016

Optical Materials EXPRESS

14. H. J. Coufal, D. Psaltis, and G. T. Sincerbox, *Holographic Data Storage*, Springer Series in Optical Sciences (Springer, 2000), Vol. 76.
15. S. Gallego, C. Neipp, M. Ortuño, E. Fernández, A. Beléndez, and I. Pascual, "Analysis of multiplexed holograms stored in a thick PVA/AA photopolymer," Opt. Commun. **281**(6), 1480–1485 (2008).
16. M. Ortuño, A. Márquez, E. Fernández, S. Gallego, A. Beléndez, and I. Pascual, "Hologram multiplexing in acrylamide hydrophilic photopolymers," Opt. Commun. **281**(6), 1354–1357 (2008).
17. Y. Qi, H. Li, J. Guo, M. R. Gleeson, and J. T. Sheridan, "Material response of photopolymer containing four different photosensitizers," Opt. Commun. **320**, 114–124 (2014).
18. K. Osabe and H. Saito, "Stability of holographic gratings recorded on photopolymer films using acrylamide as monomer and N,N′-methylenebisacrylamide," Proc. SPIE **9386**, 93860Q (2015).
19. F. Zhai, Y. Hao, and K. Yang, "Improving the holographic performance of photopolymers for holographic recording application," Optik (Stuttg.) **126**(23), 4304–4307 (2015).
20. Y. Li, C. Wang, H. Li, X. Wang, J. Han, and M. Huang, "Effect of incorporation of different modified Al2O3 nanoparticles on holographic characteristics of PVA/AA photopolymer composites," Appl. Opt. **54**(33), 9799–9802 (2015).
21. S. Hosam, N. Izabela, M. Suzanne, M. Colm, and T. Vincent, "Characterization of an acrylamide-based photopolymer for data storage utilizing holographic angular multiplexing," J. Opt. A, Pure Appl. Opt. **7**(5), 255–260 (2005).
22. M. Ortuño, S. Gallego, C. García, C. Neipp, A. Beléndez, and I. Pascual, "Optimization of a 1 mm thick PVA/acrylamide recording material to obtain holographic memories: method of preparation and holographic properties," Appl. Phys. B **76**(8), 851–857 (2003).
23. H. Kogelnik, "Coupled wave theory for thick hologram gratings," Bell Syst. Tech. J. **48**(9), 2909–2947 (1969).
24. V. Pramitha, R. Joseph, K. Sreekumar, and C. S. Kartha, "Peristrophic multiplexing studies in silver doped photopolymer film," J. Mod. Opt. **57**(10), 908–913 (2010).
25. E. Fernández, M. Ortuño, S. Gallego, C. García, A. Beléndez, and I. Pascual, "Comparison of peristrophic multiplexing and a combination of angular and peristrophic holographic multiplexing in a thick PVA/acrylamide photopolymer for data storage," Appl. Opt. **46**(22), 5368–5373 (2007).
26. A. Pu, K. Curtis, and D. Psaltis, "Exposure schedule for multiplexing holograms in photopolymer films," Opt. Eng. **35**(10), 2824–2829 (1996).
27. M. Ortuño, E. Fernández, S. Gallego, A. Beléndez, and I. Pascual, "New photopolymer holographic recording material with sustainable design," Opt. Express **15**(19), 12425–12435 (2007).
28. E. Fernández, R. Fuentes, M. Ortuño, A. Beléndez, and I. Pascual, "Holographic grating stability: influence of 4,4′-azobis (4-cyanopentanoic acid) on various spatial frequencies," Appl. Opt. **52**(25), 6322–6331 (2013).
29. R. Fernández, S. Gallego, V. Navarro-Fuster, C. Neipp, J. Francés, S. Fenoll, I. Pascual, and A. Beléndez, "Dimensional changes in slanted diffraction gratings recorded in photopolymers," Opt. Mater. Express **6**(11), 3455–3468 (2016).
30. F. T. O'Neill, J. R. Lawrence, and J. T. Sheridan, "Thickness variation of self-processing acrylamide-based photopolymer and reflection holography," Opt. Eng. **40**(4), 533–539 (2001).

1. Introduction

Photopolymers have proved to be useful in different holographic applications such as holographic data storage (HDS) or holographic optical elements (HOEs). There is an ever growing need to increase the capabilities and flexibility of data storage systems. HDS offers high storage density, fast data transfer rate and short random access time [1–3]. HOEs were introduced in the 1980's as an alternative to conventional optical elements and have several advantages over the latter. They can manipulate light in a simpler and cheaper way and at the same time are much lighter and versatile [4–7].

Holographic photopolymers were first described in 1969 as a mixture of acrylic monomers (barium and lead acrylate and acrylamide) and a photoinitiator. Typically, photopolymers are, however, composed of a total of three components: the photoinitiator, one or more monomers, and a polymeric binder. The binder provides mechanical stability and ensures good optical properties.

However, most photopolymers have certain undesirable features, such as the toxicity of some of their components or their low environmental compatibility. New trends in photopolymers include better environmental compatibility, low toxicity, ease of production and good recycling properties [8–10].

This paper follows on from previous studies in which we developed the biocompatible photopolymer 'Biophotopol' as a recording material for single holographic gratings [11,12]. In this case two different multiplexing methods were used independently and simultaneously

Optical Materials EXPRESS

in order to assess the capability of Biophotopol to obtain multiplexed holographic gratings at a single location in a 300 μm thick layers. We also compared the results with those obtained in multiplexed acrylamide/riboflavin (AA/RF) samples. This is the first time that the use of riboflavin dye as initiator system with acrylamide monomer has been reported.

It is known that the RF molecule (component of vitamin B_2) and Flavin derivatives absorb at visible wavelengths with a specific absorption peak near 450 nm. These substances are photosensitizers because they have a high intersystem crossing quantum yield [13]. Upon light absorption they reach the triplet excited state and react with electron donors to generate radical intermediates. These radicals, either from the dye molecule itself or from triethanolamine (TEA) facilitate chain polymerization through a redox reaction, as happens in the case of the yellowish eosin-triethanolamine pair.

The dynamic range of the medium is formally described as the number of single holographic gratings that can be stored in the same volume of media by multiplexing to create a DE of 100% [2,14]. It represents the storage capacity of a holographic material and is characterized by the parameter M#:

$$M\# = \sum_{i=1}^{N} DE_i^{1/2} \tag{1}$$

where DE is the diffraction efficiency of each multiplexed hologram and i'th is the number of the multiplexed hologram.

Thus, M# is a suitable measure of the possible storage capacity of a given medium, and is proportional to the thickness and the index contrast of the medium. M# determines the number of index gratings, N, that can be written in the holographic medium, and whose individual DEs can be clearly distinguished from the noise level.

Peristrophic multiplexing is a very useful tool especially when the holographic recording medium is relatively thin. It is usually implemented by combining of two or more multiplexing techniques that increase the storage density. In order to assess the capability of the Biophotopol photopolymer as a data recording material we used two different peristrophic multiplexing techniques. These techniques are commonly used in HDS experiments. In one case the rotation axis is parallel to the sample plane and thus the angle of incidence of the reference and object beams varies continuously during storage of the holograms. Each hologram is stored at an angle of incidence slightly different to that of the previously recorded one. In the other case, the rotation axis is perpendicular to the sample plane and thus the angle of incidence of the reference and object beams is constant during hologram storage. There is no loss of the previous grating when a new grating is recorded at the same point.

One of the photopolymers most widely studied is polyvinyl alcohol acrylamide (PVA/AA). It has been developed in 1 mm thick layers by our research team [15,16] and other research groups [17–20] showing its suitability as a HDS [21]. It exhibits high energetic sensitivity and diffraction efficiency. Yellowish eosin is commonly used as sensitizer with PVA/AA photopolymer. Therefore, in order to compare the results of environmentally friendly Biophotopol with those of the well-known highly toxic AA based photopolymers we used riboflavin instead of yellowish eosin (YE).

The material's temporal stability was also investigated with particular reference to the Bragg selectivity curve, DE variation and grating shrinkage variation. This was accomplished by monitoring the gratings before and after curing the sample.

2. Experimental

2.1 Preparation of the material

Photopolymer layers consist of a polyvinyl alcohol binder with a monomer (acrylamide or sodium acrylate), an electron donor, and a dye sensitizer. The composition of Biophotopol was based on that described in previous study with NaAO as the monomer [12] and it was

Optical Materials EXPRESS

optimized to obtain 300 µm thick layers. Table 1 shows the component concentrations of the Biophotopol (NaAO/RF) and acrylamide/riboflavin (AA/RF) photopolymers. The composition of the AA/RF samples used was similar to that of the NaAO/RF samples, the only difference being the monomer used. The compositions consist of water as solvent, triethanolamine (TEA) as coinitiator and plasticizer, riboflavin 5′-monophosphate sodium salt (RF) as dye and polyvinyl alcohol (PVA) as binder (Mw = 130000 g/mol, degree of hydrolysis = 87.7%) with the corresponding monomer (AA or NaAO). The quantity of AA used was calculated from previous studies in order to obtain 300 µm thick acrylamide photopolymer films giving maximum diffraction efficiency [22].

Table 1. Molarity composition of each photopolymer solution. PVA in percentage.

Sample	AA (M)	NaAO (M)	PVA (w/v)	TEA (M)	RF (M)
NaAO		0.34	13.4	$9.2\text{x}10^{-3}$	$1.0\text{x}10^{-3}$
AA	0.34		13.4	$9.2\text{x}10^{-3}$	$1.0\text{x}10^{-3}$

The photopolymer solution was deposited in circular glass molds by gravity. The molds were then left inside an incubator (Climacell 111) at controlled humidity and temperature (RH = 60 ± 5% and T = 20 ± 1 °C, respectively). When part of the water had evaporated (drying time 40 h), the "solid" film thickness decreased to 300 µm approximately. The glass molds were then ready for exposure, which took place immediately. The thickness of the solid films was measured using an ultrasonic pulse-echo gauge (PosiTector 200) after exposure.

The wavelength of the Argon laser used in the hologram recording experiments was 488 nm at which the absorption coefficient of the Biophotopol solution was 91 cm^{-1}, as demonstrated in a previous study [12].

The recorded grating is a volume grating with a Q factor [23] of 1155 >> 10 that has been calculated using the Biophotopol's data. The modulation stored in this type of materials is phase modulation. As the surface relief modulation and absorption modulation are negligible we only take into account the index of refraction modulation.

2.2 Holographic setup

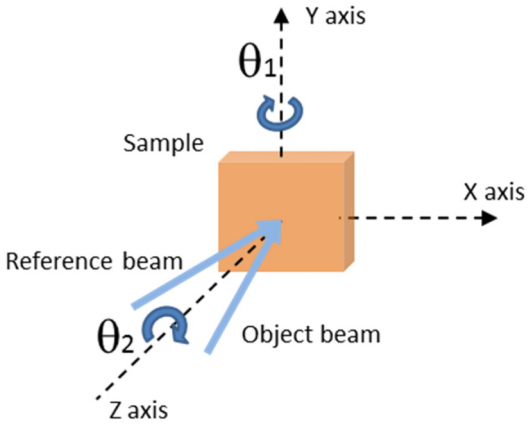

Fig. 1. Scheme of the two independent multiplexing motions.

Using the previous experimental set-up [12], multiplexed gratings were recorded at a constant exposure intensity of 3 mW/cm^2 provided by an Argon laser (BeamLok 2060 by Spectra-Physics) tuned at a wavelength of 488 nm with continuous laser exposure. The polarized beam was split into two secondary beams with an intensity ratio of 1:1 and a diameter of 1.5 cm. The angle of incidence of both the object and the reference beam at the recording

Optical Materials EXPRESS

medium were 17.1° (measured in air). This angle was used to obtain a spatial frequency of 1200 lines/mm.

For peristrophic multiplexing studies, the sample was mounted simultaneously on two motorized rotation stages. Holograms were read out with an angular resolution of 0.02°. All components (shutter, rotation stages and detectors) were connected to a computer and controlled by a LabVIEW program.

Gratings were peristrophic multiplexed by rotating the Y axis (θ_1), by rotating the Z axis (θ_2) and by rotating both axes simultaneously. As can be seen in Fig. 1 the Y and Z axes are parallel and perpendicular, respectively, to the sample plane. The system allows multiple gratings to be recorded in the same volume of material. Each grating is recorded at an angle that is Bragg mismatched from its neighboring gratings and reconstructed away from the detector, permitting a new grating to be recorded.

In order to prevent grating overlapping during the storage process the angle between consecutive gratings selected was 1° when the angle of rotation was θ_1 and 10° when the angle of rotation was θ_2. This ensures there is sufficient separation between the gratings to enable them to be subsequently reconstructed independently.

The exposure time was controlled by placing an electronic shutter in front of the Ar laser. No pre-exposure energy was used to reduce the inhibition period because the polymerization process began almost instantaneously, in both compounds. The analysis in real time of grating formation and the angular multiplexed gratings reconstruction processes were made using a HeNe laser. DE and TE (transmission efficiency) were calculated as the intensity of the diffracted and transmitted beams divided by the incident beam, respectively.

The DE data was fitted by Kogelnik's equation [23]:

$$DE = \exp\left(\frac{-\alpha \cdot d}{\cos\theta}\right) \cdot \sin^2\left(\frac{\pi \cdot n_1 \cdot d}{\lambda \cdot \cos\theta}\right) \tag{2}$$

where λ is the wavelength of reconstruction in air, α takes into account the absorption and scattering of the hologram, d is the thickness of the hologram, n_1 is the index modulation and θ is the angle of reconstruction in the recording medium, related to the angle of reconstruction in air by Snell's law.

The system was used to determine the photopolymer's M# Eq. (1) for holographic gratings recorded at a spatial frequency of 1200 lines mm^{-1}. The diffraction efficiency was taken to be the intensity of the diffracted beam divided by the input beam intensity. In general materials with large values of M# are more suitable for use as holographic data storage.

3. Results and discussion

The aim of this paper was not to determine the maximum storage capacity of the Biophotopol photopolymer but to demonstrate that it can be used to multiplex gratings with an acceptable capacity. Hence, we recorded thirteen peristrophic multiplexed gratins by rotating two different axes in two different materials –a low toxicity Biophotopol material and a high toxicity AA material. As we described in previous study [12] the Biophotopol photopolymer exhibits lower transmittance at wavelengths around 450 nm so we used an Argon laser at a wavelength of 488 nm to record the holographic gratings. Therefore, in order to be able to use the same recording wavelength for both compounds we decided to use RF as a sensitizer in the acrylamide photopolymer.

Consequently, the only difference between the compositions of the two polymeric materials was the monomer used. In the Biophotopol photopolymer the monomer is NaAO and in the acrylamide photopolymer the monomer is AA. The rest of the components are the same in both photopolymers.

Optical Materials EXPRESS

3.1. Riboflavin as a polymer initiator system

Figure 2(a) shows the UV-VIS transmittance spectrum for photopolymers with YE and RF dyes. As can be seen, the transmittance at 488 nm for the photopolymer with YE (red line) is too much higher (around 40%) to produce gratings efficiently. However, the transmittance of the AA photopolymer with RF is around 11%, low enough to record gratings with high efficiency. For this reason, we decided to use RF in both photopolymers. Figure 2(b) shows the absorption coefficient (α). At the reconstruction wavelength α = 1.1 cm^{-1}, this means that the material does not have absorption at this wavelength and therefore we can get rid of the bulk material absorption.

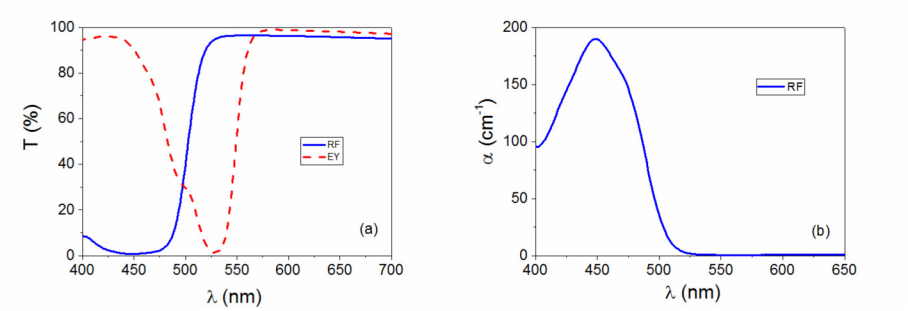

Fig. 2. Transmittance spectra (T) of the unexposed RF (solid blue line) and YE (discontinuous red line) photopolymer dyes (a) and absorption coefficient spectra of RF (b).

To study how these photopolymers, behave as holographic recording material, we recorded a diffraction grating in each of them. Figure 3 shows DE versus exposure energy for both materials. As can be seen, the DE in both cases increases monotonically and has the same shape. The minimum energy necessary to respond is practically the same for both compounds (0.01 J/cm^2 approximately). The energetic sensitivity, defined as the minimum energy required to achieve maximum diffraction efficiency (DE_m), was the same for both photopolymers (0.06 J/cm^2). The energetic sensitivity is also obtained from the E maximum derivative with the same results. The DE plotted has not saturation. At the last point of this curve the diffracted intensity started to decrease and at this moment we have turned off the recording laser.

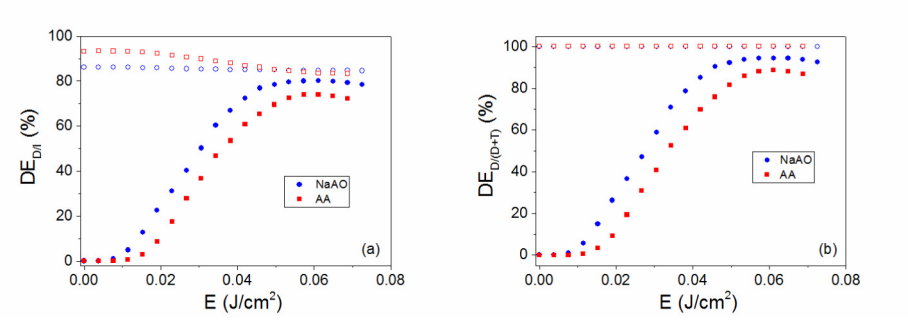

Fig. 3. Diffraction efficiency normalized to the incident intensity ($DE_{D/I}$) (a) and diffraction efficiency normalized to diffracted + transmitted intensities ($DE_{D/(D + T)}$) (b); DE (solid symbols) and DE + TE (hollow symbols) versus exposure energy (E) for both photopolymers (NaAO; blue and AA; red).

In Fig. 3 the DE + TE and DE curves are plotted. As can be seen in Fig. 3(a), the DE + TE curves show that the AA monomer has losses of around 10% due to absorption and dispersion of light as compared with around 2% in the case of the NaAO monomer, for which the sum

Optical Materials EXPRESS

DE + TE is more stable throughout the holographic recording. This indicates that the losses due to absorption and dispersion are smaller in the photopolymer with NaAO, thereby making this material more suitable for our purpose. In Fig. 3(b) the DE + TE are constant and DE curve shows the behaviour of both materials without taking account the losses.

Figure 4 shows the angular scan of both materials. In Fig. 4(a) Fresnel losses are not taken into account. In Fig. 4(b) both interfaces reflections and scattering losses are taking into account. The maximum diffraction efficiency DE_m obtained was around 80% (Fig. 4(a)) and around 95% (Fig. 4(b)). Table 2 also includes the main holographic parameters obtained from Kogelnik's coupled wave theory [23] by fitting the experimental data to Eq. (2): optical thickness (d), absorption coefficient (α), refractive index (n_0), refractive index modulation (n_1), full width at half maximum (FWHM), and the regression coefficient (R^2).

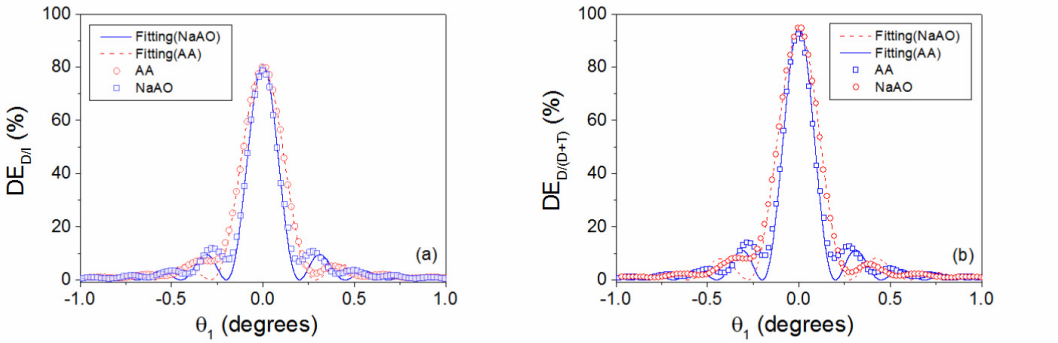

Fig. 4. Diffraction efficiency normalized to the incident intensity ($DE_{D/I}$) (a) and diffraction efficiency normalized to diffracted plus transmitted intensities ($DE_{D/(D+T)}$) (b); DE (hollow symbols) versus angular scan around the first Bragg angle (θ_1) for both photopolymers (NaAO; blue and AA; red). We have also included the fitting curves to the Kogelnik's equation (Eq. (2)) for both photopolymers.

Table 2. Main holographic parameters of the samples shown in Fig. 4.

Sample	d (μm)	α (μm^{-1})	n_0	n_1	FWHM(degrees)	R^2
AA	243	0.00086	1.502	0.0008	0.22	0.982
NaAO	300	0.00080	1.499	0.0010	0.19	0.978

The optical thickness of the NaAO sample was around 300 μm and slightly lower for the AA sample. This difference in thickness was due to the difference amounts of water retained in the drying process. Due to the ionic character of the Na^+ the polyacrylate molecules tend to retain more water by solvation than do polyacrylamide molecules. This is also shown by the FWHM parameter.

3.2. Multiplexing

As mentioned in the introduction, thirteen holograms were stored at a single location. From multiplexing studies at constant exposure time, it was seen that this type of multiplexing does not result in uniform gratings [15,24,25], which is important for holographic data storage. In all cases the exposure time used to obtain uniform diffraction efficiencies was calculated by performing an initial iteration made for each material. The exposure time for the first iteration was determined following the iterative method proposed in Ref [26]. This method is based on the application of initial schedule times, then using the diffraction efficiencies obtained, the next optimum exposure schedule is calculated. Both monomers polymerize in the same

Optical Materials EXPRESS

manner –as we already demonstrate in Ref [27] using YE as dye. To simplify the recording process, the exposure time used is the average time calculated for each material.

3.2.1 Multiplexing with axis θ_1 parallel to the sample plane

Thirteen holograms were stored at a single location rotating the axis parallel to the sample plane. This rotation causes the stored grating to be reconstructed in a horizontal direction, allowing another grating to be recorded at the same location. The exposure times and the angular positions are indicated in Table 3. Figure 5 shows DE versus the angular reconstruction for both photopolymers; we included not only the experimental data but also the theoretical data obtained from Kogelnik's coupled wave theory [23]. It may be seen that the DE of each grating in the NaAO is different and decreases as the hologram number increases, except for the two first gratings. In the case of AA based photopolymer the decrease is slower.

As can be seen the angular separation of 1° used to record the gratings is sufficient since in any case overlapping appears. The total exposure energy was 0.9 J/cm^2 for each sample. The dynamic range of Biophotopol was M# = 4.8, whereas that of the AA photopolymer was M# = 2.9. This difference is due to the high diffraction efficiencies of the holograms stored in the photopolymer with NaAO as compared with those stored in the photopolymer with AA monomer. This indicates that the variable exposure energy scheduling makes better use of the dynamic range of the NaAO photopolymer material. The lower value of M# obtained for AA photopolymer is probably due to the fact of using an averaged exposure energy scheduling instead of using a different exposure energy scheduling for each photopolymer. In a previous study [22], 700 μm thick layer of YE/AA showed a M# equal to 25.91. This higher M# value for AA photopolymer is clearly due to its higher layer thickness and a better use of the dynamic range. This demonstrates the storage capacity of Biophotopol as recording material and its potential for use as multiplexing photopolymer material.

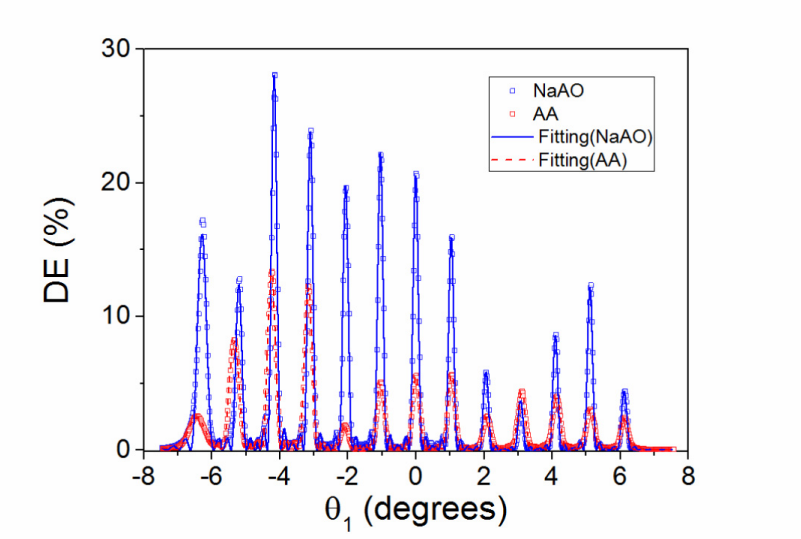

Fig. 5. Diffraction efficiency (DE) versus angular scan (θ_1) of thirteen angle-multiplexed volume holograms.

The main parameters are presented in Table 3, exposure time (t), effective optical thickness (d), absorption coefficient and refractive index modulation (n_1) of each grating plotted in Fig. 5 (the first grating stored is on the left and the last is on the right).

Optical Materials EXPRESS

Table 3. Parameters for 13 multiplexed gratings recorded with an axis parallel to the sample for NaAO and AA samples.

			NaAO				AA			
nº	θ_1(degrees)	t(s)	d(μm)	α(μm^{-1})	n_1(x10^{-5})	DE(%)	d(μm)	α(μm^{-1})	n_1(x10^{-5})	DE(%)
1	–6	2	216	0.00285	53	16	120	0.00000	25	2
2	–5	3	307	0.00595	72	12	204	0.00000	27	8
3	–4	4	354	0.00142	42	28	246	0.00000	29	13
4	–3	5	365	0.00054	30	24	252	0.00000	27	12
5	–2	6	362	0.00000	25	20	255	0.00000	10	2
6	–1	8	371	0.00000	26	22	260	0.00000	17	5
7	0	11	373	0.00000	25	21	265	0.00000	17	5
8	1	14	389	0.00000	21	16	265	0.00000	17	6
9	2	17	385	0.00347	25	6	254	0.00000	12	2
10	3	23	378	0.00714	46	4	247	0.00000	16	4
11	4	37	399	0.00000	14	9	243	0.00047	17	4
12	5	48	384	0.00000	18	12	236	0.00805	39	3
13	6	60	352	0.00699	47	4	251	0.00048	13	2

It may be seen in both materials that there is a big difference between the width of the first grating and that of the others, thus indicating that the effective optical thickness of this grating is also different to that of the others. This occurs because at the beginning the absorption is high since the dye concentration is also high. As the dye is consumed the absorption decreases and the thickness of the stored grating increases. We can see a maximum effective thickness of 265 and 399 μm for AA and NaAO, respectively, and then thickness of the subsequent gratings decreases slightly. This effect can be explained by the fact that most of the monomer is consumed and the subsequent gratings are recorded deeper in the material, where some residual monomer still remains.

The refractive index modulation decreases as the grating number increases as reported in a previous study [15].

3.2.2 Multiplexing with axis θ_2 perpendicular to sample plane

In this case thirteen holograms were stored at a single location using the axis perpendicular to the sample plane. The film was rotated around the Z axis after each recording position in steps of 10°. This rotation causes the stored grating to be reconstructed in the vertical direction, allowing another grating to be recorded at the same location. Figure 6(a) and Fig. 6(b) show DE versus angular reconstruction for AA and NaAO, respectively. The exposure times used to record the multiplexed gratings were the same as those used in section 3.2.1 to record multiplexed gratings with the axis parallel to the sample for each photopolymer sample.

As can be seen in Fig. 6 the optical thickness of the first grating in both photopolymers is lower than the others stored gratings, as we explained in section 3.2.1. This time the dynamic range achieved of Biophotopol was M# = 3.3 and that of AA was M# = 5.3, in contrast to what happened in section 3.2.1, the variable exposure energy scheduling makes better use of the dynamic range of the AA photopolymer material along the Z axis. Readjusting the exposure time scheduling will make a better use of the dynamic range of the NaAO material in this type of multiplexing.

Optical Materials EXPRESS

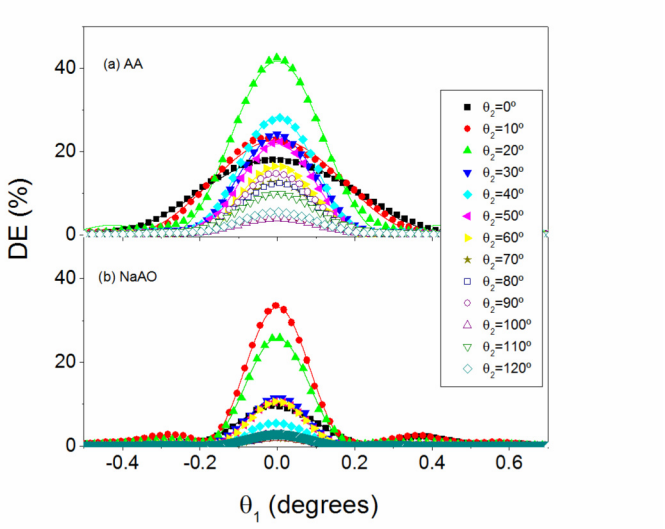

Fig. 6. Diffraction efficiency (DE) versus angle of reconstruction Y axis (θ_1) for a) AA and b) NaAO samples for different θ_2 angles along the Z axis.

Table 4. Parameters for 13 multiplexed gratings recorded with the axis perpendicular to the sample for NaAO and AA samples.

			NaAO				AA			
nº	θ_2(degrees)	t(s)	d(μm)	α(μm^{-1})	n_1(x10^{-5})	DE(%)	d(μm)	α(μm^{-1})	n_1(x10^{-5})	DE(%)
1	0	2	283	0.00001	22	10	150	0.00000	58	18
2	10	3	357	0.00001	34	33	176	0.00000	55	23
3	20	4	358	0.00001	29	26	248	0.00000	55	42
4	30	5	371	0.00001	18	12	282	0.00000	35	24
5	40	6	394	0.00001	12	6	294	0.00000	37	28
6	50	8	396	0.00001	16	11	301	0.00000	32	22
7	60	11	375	0.00000	9	3	306	0.00000	27	16
8	70	14	393	0.00000	7	2	288	0.00000	24	13
9	80	17	400	0.00001	4	1	290	0.00000	24	12
10	90	23	391	0.00000	9	3	291	0.00000	26	14
11	100	37	372	0.00000	7	2	275	0.00000	14	4
12	110	48	375	0.00000	9	3	267	0.00000	23	10
13	120	60	394	0.00001	9	3	274	0.00000	17	5

In general, the optical thickness of the NaAO material is greater than that of the AA material. As shown in Tables 1, 2 and 3, the optical thickness of the Biophotopol photopolymer is in all cases slightly greater. Moreover, in previous studies it was found that when the thickness increased the angular interval for the angular response curve decreased. A small angular interval is very important when recording many holograms by multiplexing since this makes it more difficult for holograms to overlap, thereby allowing these holograms to be reconstructed more easily especially when the rotation axis is parallel to the sample plane.

Optical Materials EXPRESS

3.2.3 Multiplexing with a combination of both methods

As already shown, the Biophotopol photopolymer has the capacity to store gratings at a single location using parallel and perpendicular multiplexing techniques separately. Now, we shall assess the Biophotopol's capacity to store twenty gratings at a single location using a combination of both multiplexing techniques.

Five gratings for each multiplexed Z axis position were stored with an angular separation of 1° along the Y axis. The angular separation between each Z axis position was 10°. In order to increase the dynamic range, we increased the number of stored gratings by adjusting the exposure times. In order to store gratings with uniform diffraction efficiency (DE), it is necessary to decrease the exposure times for the first holograms and increase the exposure times for the last ones.

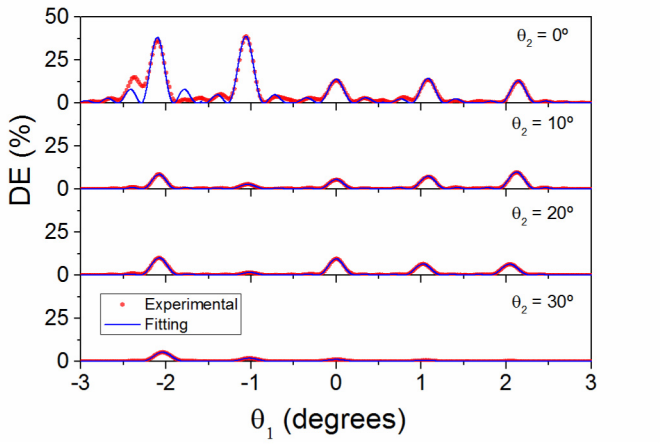

Fig. 7. Grating diffraction efficiency (DE) versus Y and Z axes (θ_1 and θ_2, respectively).

Figure 7 shows the DE of the multiplexed gratings using both multiplexing methods together and Table 4 shows the main parameters of the twenty gratings stored. The accumulated dynamic range obtained for the Biophotopol sample was M# = 5.5. Despite optimizing the time scheduling and obtaining a better dynamic range we observed that the two first gratings had a higher DE than the others. In order to improve the uniformity of the DE of the stored gratings we can reduce the exposure time of the two first gratings and slightly increase the exposure time of the last ones.

It may be seen in Table 5 that for each perpendicular multiplexing position the optical thickness of the stored parallel gratings is similar and around 300 μm, except for the last perpendicular position where the optical thickness decreased as the number of the grating increased. This can be explained by the lack of monomer which had polymerized during the recording of previous gratings.

Thus, with a combination of the two types of multiplexing a greater number of holograms may be stored without overlapping. Once more, these results demonstrate the capability of Biophotopol photopolymer as holography recording material for multiplexing applications with the advantages of its environmentally compatible properties.

Optical Materials EXPRESS

Table 5. Parameters of 20 multiplexed gratings recorded with a combination of perpendicular and parallel axes.

nº	θ_1(degrees)	θ_2(degrees)	t(s)	d(μm)	α(μm^{-1})	n_1(x10^{-5})	DE(%)
1	–2	0	2	305	0.00256	125	38
2	–1	0	2	297	0.00307	107	39
3	0	0	2	278	0.00628	139	14
4	1	0	3	304	0.00596	118	14
5	2	0	4	318	0.00604	81	13
6	–2	10	4	322	0.00730	86	9
7	–1	10	5	273	0.01240	130	3
8	0	10	6	305	0.00910	97	6
9	1	10	8	295	0.00850	100	7
10	2	10	11	300	0.00703	79	10
11	–2	20	14	304	0.00605	62	10
12	–1	20	17	297	0.01355	110	2
13	0	20	23	321	0.00246	29	10
14	1	20	37	307	0.00652	51	7
15	2	20	48	291	0.00651	49	6
16	–2	30	60	281	0.00170	21	5
17	–1	30	60	260	0.01468	101	2
18	0	30	65	255	0.01696	108	1
19	1	30	75	242	0.02037	115	1
20	2	30	80	193	0.02949	202	0

3.3 Grating stability

Biophotopol's stability was determined doing the reconstruction of the holograms and analyzing the variation of the maximum diffraction efficiency (DE_m) over the time. For this purpose, thirteen holograms were stored at a single location using the axis parallel to the sample plane. In this case, the film was rotated around the Y axis after each recording position in steps of 3°. We decided to increase the grating separation in order to make it easier to analyze and discriminate each grating DE peak versus time.

The gratings were recorded along the Y axis, from zero to the end alternately from right to left. In this case the time schedule was the same as in section 3.2.1 and 3.2.2. However, the aim of this section was not to evaluate the uniformity but rather the evolution of the maximums obtained.

After recording the grating not all the dye in the photopolymer is consumed and the reaction continues if the hologram is exposed to incoherent light. One way to avoid this reaction is to remove the excess dye after recording the grating. Therefore, after the initial reconstruction (t = 0 h), we exposed the sample to a 13.5 W (875 lumen at 6500K) LED lamp for 20 minutes. This curing process does not erase the grating because the dye that remains in the exposed zones is negligible. This process only affects the remaining dye in the unexposed zones and therefore the grating renders more stable over time. The cured gratings were stored in laboratory conditions where the temperature and relative humidity change.

We only analyzed the first seven recorded gratings since the rest had lower DE_m which made it difficult to determine them with sufficient accuracy. Figure 8 shows the DE_m of each multiplexed grating versus angular reconstruction at five different times. For the first 1653

Optical Materials EXPRESS

hours the DE_m of the gratings hardly changed with time. At 2759 hours the DE_m decreased and the angular position of the gratings changed due to increasing temperature and decreasing relative humidity. At the same time, there was a displacement of the peak positions towards higher absolute angular values. At 3143 hours the initial DE_m values were restored as well as the initial position of the peaks by decreasing the temperature and increasing the relative humidity.

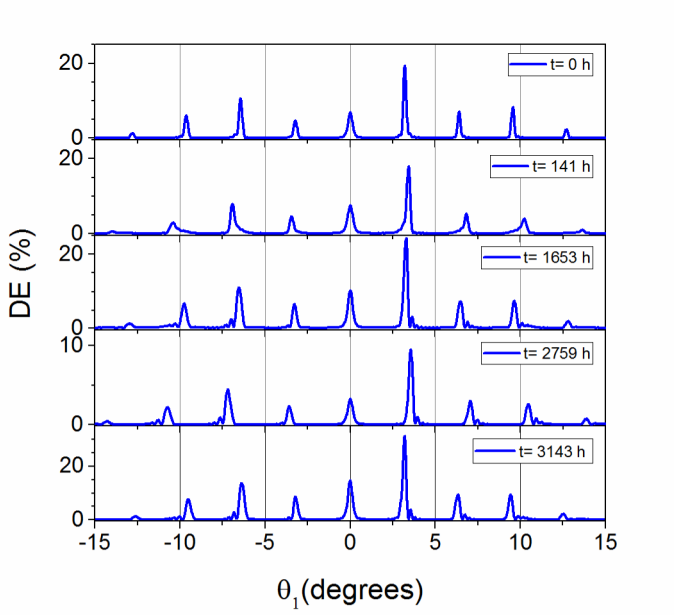

Fig. 8. Angular reconstruction of multiplexed gratings along the Y axis (θ_1) at different times (t).

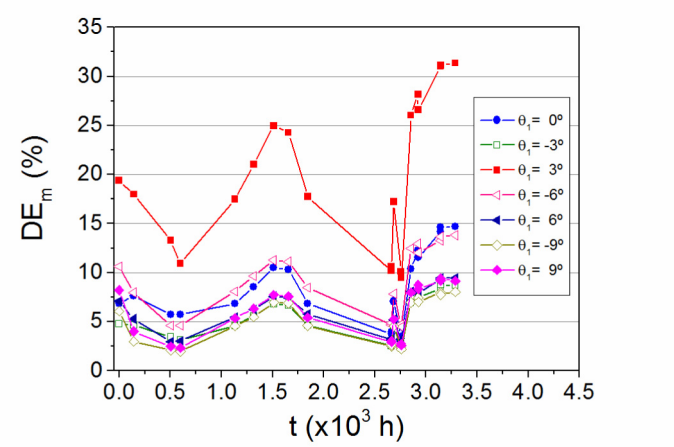

Fig. 9. Maximum diffraction efficiency (DE_m) versus reconstruction time (t) for each grating.

Figure 9 shows the evolution of DE_m versus time in more detail. All the curves on this graph have the same shape, which indicates that the gratings evolve in the same manner. As we can see, the DE_m changes over time and this variation depends on the initial DE_m value. The higher the initial DE_m value is the greater variation over the time produce. The DE_m for each grating changes over the time but this variation is greater for $\theta_1 = 3°$ geometry, which

Optical Materials EXPRESS

have an initial DE_m higher than the other gratings. The DE_m was found to increase when the temperature decreased and relative humidity increased. Therefore, it was possible to restore or even increase the initial DE_m by changing the values of temperature and relative humidity. The AA photopolymer gratings did not exhibit this property, see Ref [28]. These variations could allow us to use Biophotopol photopolymer as a sensor.

In Fig. 10, shows the angular displacement ($\Delta\theta_m$) of DE_m versus time. This displacement is related to shrinkage as we assessed and quantified in other studies [29,30]. Firstly, $\Delta\theta_m$ is close to zero for the grating stored at the zero position ($\theta_1 = 0°$). Gratings stored to the right and left of the zero position present a variation in $\Delta\theta_m$ and this variation is symmetrical relative to the zero position. $\Delta\theta_m$ increases as DE_m decreases and vice versa.

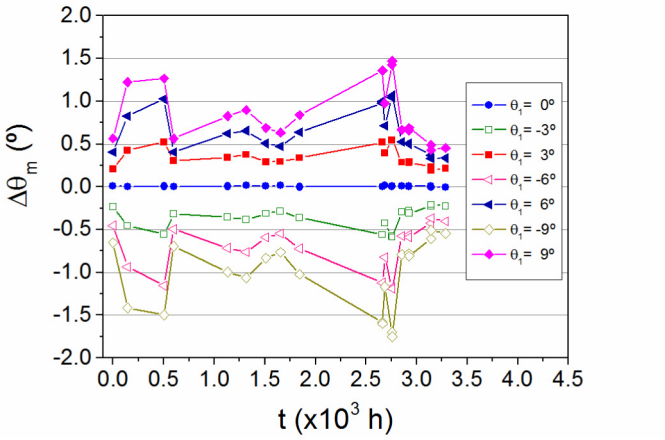

Fig. 10. Angle shift of the maximum DE versus reconstruction time (t) for each grating.

Figure 11 shows two photographs of Biophotopol samples. Both have two visible gratings oriented in the Bragg direction to the fluorescent tubes so that the color composition of the diffracted light may be seen. The first photograph shows an uncured Biophotopol sample with (a) one stored grating and (b) thirteen stored multiplexed gratings along the Y axis. The yellow color observed in the sample is due to the residual dye.

The second photograph shows a cured Biophotopol sample with (c) one stored grating and (d) thirteen stored multiplexed gratings along the Z axis. There are other gratings stored in the samples at different positions but they are not visible because of the great angular selectivity and high transparency of the Biophotopol photopolymer gratings, as can be seen in both photographs in Fig. 11.

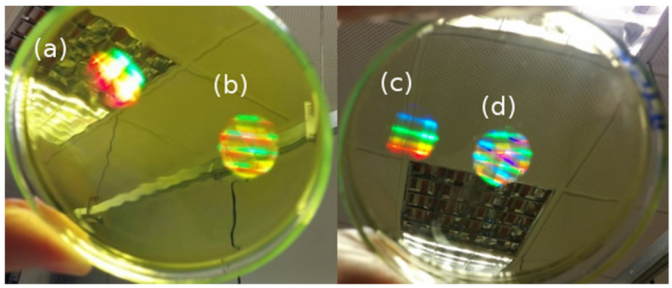

Fig. 11. Photograph of an uncured recorded sample with (a) one unslanted grating and (b) thirteen multiplexed gratings along the Y axis and a cured recorded sample with (c) one unslanted grating and (d) thirteen multiplexed gratings along the Z axis.

Optical Materials EXPRESS

4. Conclusions

We obtained multiplexed diffraction gratings in 300 μm thick layers of Biophotopol and AA based photopolymers using two different types of multiplexing. Riboflavin was the dye used in the two photopolymers layers and thirteen gratings were recorded in both. When the multiplexing axis was parallel to the sample plane the dynamic range, M#, of the Biophotopol layers was 4.8 and that of the AA material was 2.9. On the other hand, when the multiplexing axis was perpendicular to the sample plane M# was 3.3 in the Biophotopol layers and 5.3 in the AA layers. Using a combination of the two multiplexing techniques, twenty gratings were stored in Biophotopol whose M# reached 5.5. This demonstrates that both materials can be used in HDS and that it is even possible to storage several HOEs in the seam layer. In future studies we will develop our Biophotopol material for uses as a holographic memory by optimizing the time schedule in order to increase the number of gratings stored with similar DE.

The study of the stability of the Biophotopol layers was done over a period of four months. The DE_m values fluctuated around the initial DE_m values. This variation depended on the initial DE_m and the temperature and relative humidity conditions.

In this study we demonstrated the storage capacity of Biophotopol as a recording material together with its potential application as multiplexing photopolymer material. Its performance is comparable to that of to the AA based photopolymer in this type of applications, with the added advantage of its low toxicity.

Funding

Ministerio de Economía y Competitividad (Spain) (FIS2014-56100-C2-1-P and FIS2015-66570-P); Generalitat Valenciana (Spain) (PROMETEO II/2015/015).